Impacts of Climate Change and Land-Use Change on Hydrological Processes and Sediment Load in the Upper Cau River Basin, Northern Vietnam

Ngoc Anh, N.,[1*] Van Trung, C.,[1] Hong Gam, N. T.,[1] Duc Vinh, H.[2] and Trung, N. H.[1,3]
[1]Faculty of Resource Management, University of Agriculture and Forestry – Thai Nguyen University, Thai Nguyen, Vietnam, E-mail: nguyenngocanh@tuaf.edu.vn*
[2]Key Laboratory of River and Coastal Engineering, Vietnam Academy for Water Resources, Hanoi, Vietnam
[3]Mathematics and Geospatial Science, RMIT University, Melbourne, VIC 3000, Australia
**Corresponding Author*

DOI: https://doi.org/10.52939/ijg.v22i4.4941

Abstract
Climate change and land-use change strongly influence hydrological processes and soil erosion in tropical mountainous watersheds. This study uses the SWAT model to assess their individual and combined impacts on streamflow, sediment, and soil erosion in the Upper Cau River Basin, northern Vietnam. The model was calibrated and validated using observed hydro-meteorological data for 1997–2020 and applied to scenario-based projections of future climate (2021–2050) and land-use planning to 2050. The SWAT model demonstrated high predictive accuracy for both streamflow and sediment (NSE > 0.76, R^2 > 0.77). Results indicate that, relative to the baseline, the combined climate and land-use change scenario produces the largest impacts, with mean streamflow increasing by 44.95%, sediment discharge at the gauge station rising by 53.3%, and average basin-wide soil erosion reaching 12.57 t/ha/year more than a 379% increase. By comparison, climate change alone increases mean streamflow and soil erosion by 44.8% and 73.7%, respectively, while land-use change alone causes only minor changes in streamflow (+0.82%) but substantially increases soil erosion (+265%). These findings demonstrate a pronounced amplification of hydrological extremes and erosion risk when both drivers act together. Beyond scenario comparison, this study contributes a spatially explicit erosion hotspot attribution framework that links scenario forcing to hydrological response unit and sub-basin prioritisation of erosion risk. Spatial analysis reveals a basin-wide shift from predominantly low erosion under baseline conditions to widespread moderate and high erosion under the combined scenario. While the results highlight the dominant and interacting roles of climate and land-use change, they reflect SSP2-4.5 projections from a single climate model (UK Earth System Model, UKESM1-0-LL), and uncertainty across multiple climate models was not considered. The findings provide a robust scientific basis for targeted watershed management and erosion-control planning in northern Vietnam's mountainous regions.

Keywords: Climate Change, Hydrology, Land-Use Change, Sediment Load, Upper Cau River Basin

1. Introduction

Climate change and land-use change are widely recognised as primary drivers that strongly influence watershed-scale hydrological processes and soil erosion. Climate change alters temperature regimes, precipitation patterns, and the frequency and intensity of extreme rainfall events, while land-use transitions such as deforestation, agricultural expansion, and urbanization reduce vegetation cover, decrease infiltration capacity, and increase surface runoff, thereby directly affecting water balance, sediment transport, and erosion dynamics [1][2][3] and [4]. In tropical regions, particularly in mountainous watersheds, land-use/land-cover changes associated with forest degradation further intensify runoff generation and pollutant transport, amplifying erosion processes and disrupting hydrological regulation [2][3][5] and [6]. Tropical forests play a critical role in maintaining watershed ecological integrity [7]; however, severe land-cover degradation often leads to more frequent and intense runoff and erosion events with substantial impacts on water balance and sediment delivery [2][3] and [6]. Numerous empirical studies worldwide have demonstrated that the combined influence of climate change and land-use change can markedly amplify hydrological extremes and erosion responses [3] and

[4]. For example, in the Upper Mara River Basin (Kenya), reductions in vegetation cover due to land-use change led to significant increases in sediment transport when variable rainfall inputs were incorporated into hydrological simulations [8]. In Pakistan, combined forest loss, expansion of bare land, and climate change resulted in enhanced extreme runoff and severe soil erosion [9]. Similar responses have been reported in agricultural and subtropical basins [2][6][9] and [10]. A recent study [11] further emphasized that poorly managed land use characterised by reduced vegetation cover, agricultural expansion, and bare soil exposure can substantially increase soil erosion, particularly in sensitive sub-watersheds. Together with the anticipated intensification of extreme rainfall under future climate conditions, these land-use pressures are expected to exacerbate soil loss and sediment yield, posing increasing challenges for sustainable watershed management [10][12][13] and [14].

Studies indicate that hydrological models such as the Soil and Water Assessment Tool (SWAT) have been widely used to analyse the impacts of climate and land-use changes [15] and [16]. These studies have helped elucidate the responses of streamflow, surface runoff, infiltration, soil retention capacity, and sediment transport within watersheds. In Vietnam, climate variations, including increased air temperature and more pronounced changes in rainfall [17], along with agricultural and industrial development and population growth [18], have significantly affected soil erosion and water resources. However, while previous studies exist in Vietnam, few have integrated future land-use planning scenarios (up to 2050) with future climate projections (2021–2050) to assess the combined impacts of climate change and human activities on hydrological processes and sediment yield, particularly in the northern midland and mountainous regions [19]. This gap is especially evident in the Upper Cau River Basin, where complex topography, dynamic vegetation cover, and diverse land-use patterns strongly influence runoff generation and sediment transport processes [20]. Moreover, modelling climate change and land-use change separately may underestimate total sediment yield, as such approaches fail to capture the non-linear and synergistic interactions between intensified rainfall, vegetation degradation, and altered surface runoff pathways. Addressing this limitation, the present study integrates future climate projections for 2021–2050 with land-use planning data projected to 2050 to quantify the individual and combined effects of climate change and land-use change on streamflow, sediment transport, and soil erosion in the Upper Cau River Basin.

Despite growing recognition of the combined impacts of climate change and land-use change, integrated assessments remain limited in Vietnam, particularly for mountainous river basins characterised by complex terrain and rapid land-use transitions. The Upper Cau River Basin represents a critical case study due to its steep topography, heterogeneous land-cover patterns, and high sensitivity to hydrological extremes. In recent years, the basin has experienced several severe flood events, including record-breaking floods in 2024 and 2025, which exposed the vulnerability of existing land-use practices and watershed management strategies. These events highlight the urgent need for spatially explicit analyses that integrate future climate projections with planned land-use changes to better understand runoff generation, sediment dynamics, and erosion hotspots. However, to date, no study has systematically combined official land-use planning data with downscaled climate projections to evaluate their joint impacts on hydrology and soil erosion in the Upper Cau River Basin.

From a geoinformatics perspective, this study aims to advance an integrated spatial modelling framework that combines multi-source geospatial data with future climate projections and official land-use planning scenarios. By linking SWAT outputs with GIS-based spatial analysis at sub-basin and HRU scales, this study explicitly quantifies the combined and non-linear impacts of climate change and land-use change on hydrological and sediment processes, and identifies future erosion hotspots to support spatial planning and watershed management in mountainous regions.

Building upon our previous work that modelled streamflow and sediment yield in the Upper Cau River Basin using the SWAT model [20] and [21], this research advances an integrated geoinformatics framework by combining official land-use planning data to 2050 with downscaled CMIP6-VN (the Coupled Model Intercomparison Project Phase 6 for Vietnam [22]) climate projections to support spatially explicit erosion hotspot identification and prioritization. To achieve these objectives, the study aims to: (i) calibrate and validate the SWAT model for streamflow and sediment using observed hydrometeorological data; (ii) simulate baseline (S1) and future scenarios representing land-use change (S2), climate change (S3), and their combined effects (S4); (iii) quantify changes in streamflow, sediment load, and soil erosion under individual and combined scenario drivers; (iv) map and rank soil erosion hotspots at sub-basin and HRU scales to support spatial intervention prioritization; and (v) discuss implications for watershed management, land-use

planning, and model limitations under future climate and development pressures.

2. Study Area

The Upper Cau River Basin covers approximately 3,300 km², lying entirely within the administrative boundary of Thai Nguyen Province following its merger with Bac Kan (Figure 1). The Cau River originates in the northwestern part of the province, flows through the central region, and drains toward the Cha hydrological station (21.3725°N, 105.9208°E) as part of the Thai Binh River system [23] and [24]. The basin is characterized by a predominantly mountainous terrain with elevations ranging from about 50 m to over 1,500 m above sea level, steep and highly dissected slopes, and uneven vegetation cover, resulting in low water retention capacity and high susceptibility to soil erosion, flash floods, and landslides during the rainy season. To support the SWAT modelling process, basin slopes derived from a 30 m digital elevation model were classified into five slope classes (0–8°, 8–15°, 15–25°, 25–35°, and >35°). The model outlet was located at 21.43637°N, 105.961462°E, approximately 22 km southeast of the Gia Bay station, representing the downstream limit of the basin. The basin is characterised by a humid tropical monsoon climate, with mean annual rainfall ranging from 1,600 to 2,400 mm [24]. Approximately 80% of the total rainfall occurs during the rainy season (May - October), intensifying surface runoff and sediment transport and often causing severe floods with high peak discharges. Meanwhile, the dry season (November - April) features significantly reduced flow (Figure 2) [4]. Over the past decades, the Upper Cau River Basin has experienced several major floods. Peak flood events recorded at the Gia Bay station in 1959, 1968, 1971, 1983, and 1986 have long been considered important hydrological reference points [25]. Another major flood in 2001 reached a water level of 28.08 m. On 9th September 2024, the peak flood induced by Typhoon Yagi reached 28.81 m, surpassing all previous historical records. Most recently, on 8th October 2025, the peak flood caused by Typhoon Matmo exceeded the 2024 level by approximately 1.5 m, setting the highest flood stage ever recorded in the area [13] and [26]. These post-2020 events are presented for contextual purposes only and were not used in model calibration or validation, which was based on observed data from 1990–2020.

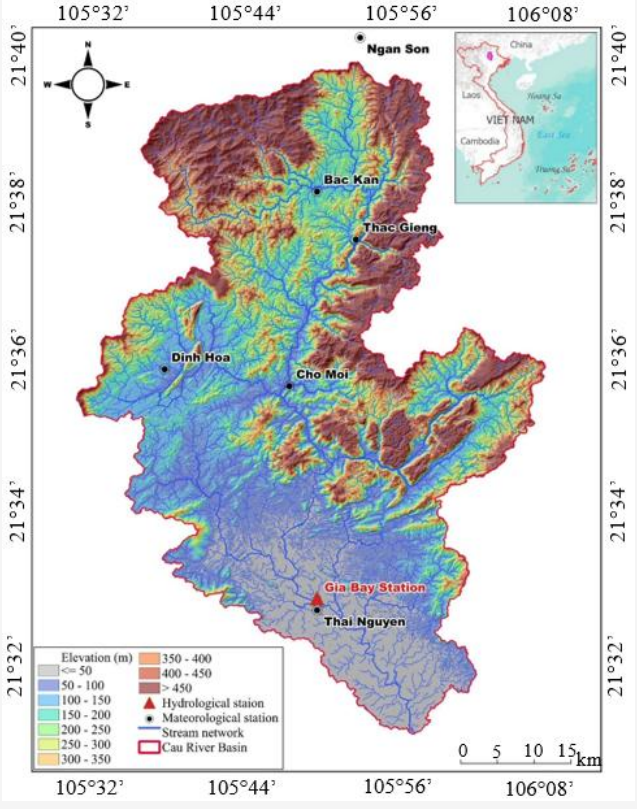

Figure 1: Study area in the Upper Cau River Basin, northern Vietnam. The Cau River is represented as the thick blue line

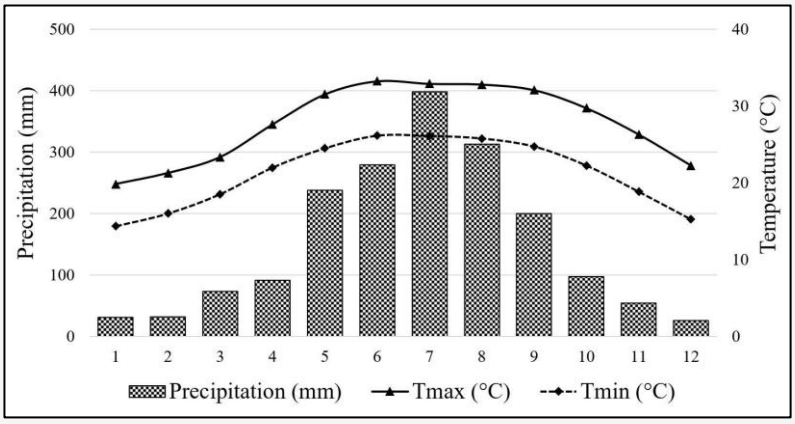

Figure 2: Mean monthly precipitation and temperature regime in the Upper Cau River Basin during the baseline period (1990–2020)

Additionally, prolonged rainfall events in 2013 and 2017 elevated flood peaks, posing inundation risks and damaging infrastructure in the midstream and downstream regions [27]. These events underscore the high hydrological sensitivity of the basin and highlight the need for hydrological modelling to support water resources planning, flood management, and climate change adaptation [3][4][13] and [28].

Historically, forests have been the dominant land-cover type in the Upper Cau River Basin; however, over recent decades, land-use transitions associated with logging, agricultural expansion, and urban development have gradually reduced forest cover and altered landscape structure [29]. In the upstream areas, shifting cultivation practices and the expansion of industrial crops have contributed to localised forest degradation and increased susceptibility to soil erosion. In the midstream and downstream regions, ongoing urbanization has progressively converted forest and agricultural land into built-up areas, increasing impervious surface coverage and influencing surface runoff and sediment delivery processes [30]. Although the overall decline in forest cover at the basin scale is moderate, these land-use changes are spatially concentrated and, when combined with climate change–driven increases in extreme rainfall, flash floods, and landslide occurrence, heighten the basin's vulnerability to hydrological alteration and sediment transport. These dynamics underscore the importance of detailed hydrological modelling to evaluate the combined impacts of climate change and land-use change in support of flood risk management, erosion control, and sustainable watershed development.

3. Methodology

The key processing steps used to assess the impacts of climate change and land-use change on hydrological processes and sediment load in the Upper Cau River Basin are presented in Figure 3 and described in detail below.

3.1 Data and Pre-Processing

This study integrates multi-source spatial datasets and long-term hydro-climatic observations within a GIS–SWAT modelling framework to simulate streamflow and sediment dynamics in the Upper Cau River Basin. A summary of the datasets used is provided in Table 1. All spatial datasets were harmonised to a common coordinate reference system (WGS84/UTM Zone 48N) and resampled to a common spatial resolution of 30 m prior to model integration to ensure consistency in analysing their combined effects on streamflow and sediment yield. Hydrological data (streamflow and suspended sediment observations) at the Gia Bay station for 1997–2020 were used for model calibration and validation. This station represents the only long-term streamflow and sediment monitoring site in the basin; therefore, internal sub-basin validation was not feasible due to data limitations.

Meteorological observations for 1990–2020 include daily rainfall from six stations (Dinh Hoa, Thai Nguyen, Cho Moi, Thac Gieng, Bac Kan, and Ngan Son) and daily temperature from two stations (Bac Kan and Thai Nguyen) (Figure 1). Although the density of meteorological stations is limited, the selected rainfall and temperature stations adequately represent the basin's dominant elevation and climatic gradients. Their use is consistent with previous hydrological studies conducted in the Cau River system [20] and [21]. Future climate projections for 2021–2050 were obtained from the CMIP6-VN dataset, which was developed from an ensemble of 35 global climate models participating in the CMIP6 framework [22].

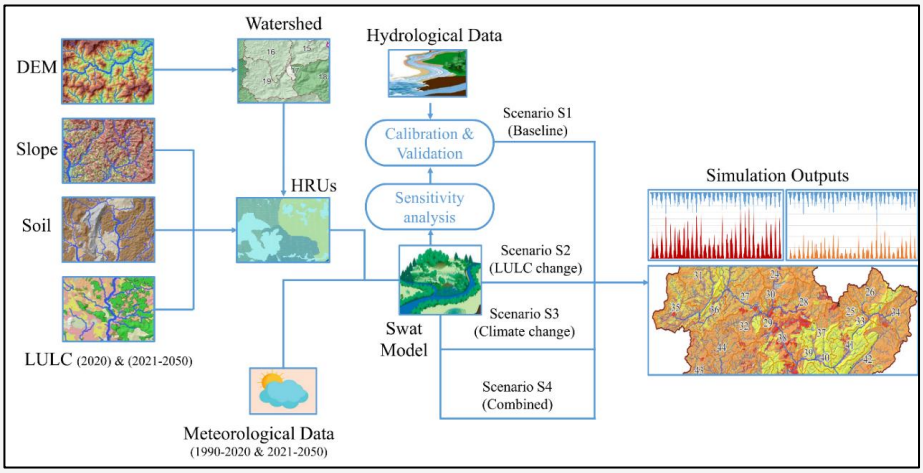

Figure 3: Methodological framework of the study

Table 1: Summary of datasets used in the SWAT model

Group	Data	Spatial/temporal resolution	Time period	Source
Hydrological	Streamflow	Gia Bay station, daily	1997–2020	Vietnam Meteorological and Hydrological Administration
	Suspended sediment	Gia Bay station, daily	1997–2020	
Meteorological	Rainfall	6 stations, daily	1990–2020	
	Air temperature	2 stations, daily	1990–2020	
Climate projection	CMIP6-VN	~10 km	2021–2050	Scientific Data [22]
Topographic	Digital elevation model	30 m	–	USGS Earth Explorer
Land-use	Current land-use map	Scale 1:100,000	2020	Provincial governments
	Land-use planning map	Scale 1:100,000	2021–2050	
Soil	Soil type map	Scale 1:100,000	2005	

The dataset provides bias-corrected climate data tailored for Vietnam. Its generation involved two main steps: (i) bias correction using the Quantile Mapping method to reduce systematic differences between model simulations and observed data; and (ii) spatial downscaling from the global model grid (~100 km) to a finer resolution of 0.1° (~10 km), using multiplicative scaling for precipitation and bilinear interpolation for temperature. The bias correction process utilised observed records from 481 rainfall stations and 147 temperature stations across Vietnam [22]. Although the CMIP6-VN dataset is based on a multi-model ensemble, this study used the UK Earth System Model (UKESM1-0-LL) [31] under the SSP2-4.5 scenario as a representative climate projection due to its documented performance in reproducing temperature and precipitation patterns over Southeast Asia. Using a single model ensures consistency across scenario simulations; however, uncertainty associated with single-model projections is acknowledged.

Topographic data, including elevation and slope, were derived from a 30 m resolution Digital Elevation Model (DEM), freely available from the USGS Earth Explorer platform [32] and [33]. The DEM was hydrologically corrected using a sink-filling procedure to remove spurious depressions. Land-use data consisted of a 2020 land-use map and a 2021–2030 Land Use Planning map (with a 2050 projection). These are official products developed by Thai Nguyen and Bac Kan provincial governments through the compilation of cadastral records and field surveys [34]. The original planning map, containing 48 land-use classes, was reclassified into 11 SWAT land-use types (agricultural, barren, forest, orchard, rice, commercial, industrial, institutional, residential, transportation, and water), using a standardised land-use cross-walk table to ensure compatibility with SWAT model requirements [21] and [35].

Soil information plays a fundamental input to the SWAT model, influencing hydrological processes such as infiltration, surface runoff, erosion, and the transport of dissolved materials [15][36] and [37]. This study used a 1:100,000 scale soil type map developed in 2005 by the provincial governments. Soil physical parameters required by SWAT, including soil depth, available water capacity

(AWC), and the soil erodibility factor (K), were assigned using national soil attribute tables and harmonized with the SWAT soil database following standard model requirements.

3.2 Simulations of Streamflow and Sediment with SWAT Model

In this study, the SWAT modelling workflow consisted of four main steps, as outlined in [20] and [21]. First, the watershed was delineated using the pre-processed DEM to generate the river network and sub-basin structure. Stream networks were delineated using a flow accumulation threshold of 2,000 ha, which controls watershed discretization and strongly influences surface runoff generation and erosion processes [15] and [36]. Second, Hydrological Response Units (HRUs) were defined by overlaying land-use, soil, and slope layers, allowing spatial representation of land-use and soil heterogeneity within each sub-basin. Third, the model simulated key hydrological processes, including surface runoff, evapotranspiration, soil water balance, and sediment yield using the Modified Universal Soil Loss Equation (MUSLE) as defined in Equation 1 [35]:

$$Sed = 11.8\left(Q_{surf} Q_{peak} A_{hru}\right)^{0.56} K \cdot C \cdot P \cdot LS \cdot CFRG$$

Equation 1

Where:

Sed = sediment yield from an HRU for a given day (t)
Q_{surf} = surface runoff volume (mm)
Q_{peak} = peak runoff rate (m^3/s)
A_{hru} = HRU area (ha)
K = soil erodibility factor
C = cover and management factor
P = support practice factor
LS = topographic factor (slope length and steepness)
$CFRG$ = coarse fragment factor (dimensionless).

Finally, the model was calibrated and validated against observed streamflow and sediment data at the Gia Bay station before being applied to baseline and future scenario simulations (section 3.3.3) to assess the individual and combined impacts of climate change and land-use change. HRUs were defined using threshold values of 5% for land-use, 5% for soil type, and 5% for slope class, which allowed the exclusion of minor landscape units while preserving the dominant hydrological characteristics within each sub-basin. Daily meteorological inputs included rainfall and temperature (maximum and minimum) data. The model was initially developed for the period 1990-2020, with the first three years used as a warm-up period, following the standard SWAT modelling framework [38]. To enhance model reliability, a parameter sensitivity analysis was performed using SWAT-CUP (SWAT Calibration and Uncertainty Procedures) software (version 5.1.6.2). This process was conducted on 10 key parameters influencing streamflow and 7 parameters affecting sediment yield (Table A1). Parameters were selected based on hydrological relevance in tropical monsoon basins and prior SWAT studies [4][39][40] and [41].

Given the availability of daily observed streamflow and sediment data from 1997 to 2020, the model was calibrated for 1997-2008 using the SUFI-2 (Sequential Uncertainty Fitting Version 2) algorithm [41]. The optimised parameters from this calibration were subsequently applied to simulate streamflow and sediment yield for 2009-2020, during which model performance was validated using independent observations. This 12-year calibration period ensured representation of multiple wet and dry cycles. Model performance was assessed at the monthly time step using the Nash-Sutcliffe Efficiency (*NSE*), coefficient of determination (R^2), Percent Bias (*PBIAS*), and Root Mean Square Error to Standard Deviation Ratio (*RSR*) [41] and [42]. These metrics were computed using Equations 2 to 5:

$$NSE = 1 - \frac{\sum_{i=0}^{n}\left(X_{obs,i} - X_{sim}\right)^2}{\sum_{i=0}^{n}\left(X_{obs,i} - X_{obs}\right)^2}$$

Equation 2

$$PBIAS = 100 \times \frac{\sum_{i=0}^{n}\left(X_{obs} - X_{sim}\right)_i}{\sum_{i=0}^{n}\left(X_{obs,i}\right)}$$

Equation 3

$$R^2 = \frac{\left[\sum_{i=0}^{n}\left(X_{obs,i} - \bar{X}_{obs}\right)\left(X_{sim,i} - \bar{X}_{sim}\right)\right]^2}{\sum_{i=0}^{n}\left(X_{obs,i} - \bar{X}_{obs}\right)^2 \cdot \sum_{i=0}^{n}\left(X_{sim,i} - \bar{X}_{sim}\right)^2}$$

Equation 4

$$RSR = \frac{\sqrt{\sum_{i=0}^{n}\left(X_{obs} - X_{sim}\right)_i^2}}{\sqrt{\sum_{i=0}^{n}\left(X_{obs,i} - \bar{X}_{obs}\right)^2}}$$

Equation 5

Where, X_{obs} and X_{sim} are the observed and simulated values of the hydrological and sediment variables, respectively. Model performance was considered acceptable when the following criteria were satisfied: $NSE > 0.5$, $R^2 > 0.7$, $PBIAS$ within ±15% for streamflow and ±50% for sediment, and $RSR < 0.5$ [42].

3.3 Scenario Development and Simulation

3.3.1 Climate change scenario

The climate change scenario used in this study was developed based on the CMIP6-VN climate dataset. The dataset provides key climate variables, including precipitation and temperatures (maximum and minimum), for the period 1980–2099 in NetCDF format and supports multiple emission scenarios (SSP1-2.6, SSP2-4.5, SSP3-7.0, and SSP5-8.5). In this study, the SSP2-4.5 scenario was selected to represent a moderate socioeconomic development pathway, and future climate projections were derived from the UKESM1-0-LL global climate model. This model was selected due to its documented ability to reproduce regional temperature and precipitation characteristics over Southeast Asia and Vietnam, including improved representation of seasonal rainfall variability and monsoon dynamics compared to many other CMIP6 models. Comparative evaluations within the CMIP6-VN framework indicate that UKESM1-0-LL performs favourably in capturing observed climatic patterns in the region, making it suitable for impact-assessment studies in northern Vietnam [22].

Projected climate variables for 2021-2050 were extracted for meteorological stations within the study area from the CMIP6-VN gridded dataset. Climate variables at station locations were derived using the nearest-neighbour interpolation method, ensuring consistency between gridded climate projections and point-based meteorological inputs required by the SWAT model. These data were then used to simulate future streamflow and sediment dynamics and to assess the potential impacts of climate change on hydrological processes within the basin.

3.3.2 Land-Use change scenario

The land-use change scenario was developed based on the Land Use Planning map, after extracting the area corresponding to the Upper Cau River Basin. The scenario was designed to maintain the total basin area (330,041.77 ha) while adjusting the proportions of land-use categories according to the planning orientation. The use of legally adopted land-use planning maps differentiates this study from analyses based on hypothetical or assumed land-use scenarios, providing policy-relevant and spatially explicit representations of future land-use change that are consistent with official development strategies.

As presented in Table 2, this scenario reflects the ongoing trend of converting agricultural and forest land to urban and non-agricultural uses, consistent with the region's socio-economic development strategy. Compared with the 2020 baseline, the area of paddy rice is projected to decrease from 31,588.90 ha to 25,236.69 ha (-6,352.21 ha; -1.92%), and forest land from 246,974.64 ha to 236,086.89 ha (-10,887.75 ha; -3.30%). Other agricultural land is expected to decline slightly from 16,985.43 ha to 15,803.93 ha (-1,181.50 ha; -0.36%), while unused land will reduce by 698.70 ha (-0.21%). In contrast, residential land will expand from 23,130.56 ha to 29,353.95 ha (+6,223.39 ha; +1.89%), and non-agricultural land will increase substantially from 8,760.28 ha to 21,657.05 ha (+12,896.78 ha; +3.91%). Although the overall reduction in forest cover under the planning scenario is moderate at the basin scale, the changes are spatially concentrated and, when combined with future climate variability, may exert disproportionate effects on runoff generation and soil erosion.

Even modest shifts in land-use composition, particularly reductions in forest cover and expansion of impervious or non-agricultural land, can produce non-linear increases in runoff and erosion, especially where these transitions occur on steep slopes or in erosion-prone sub-basins. These land-use projections were incorporated into the SWAT model to evaluate their future impacts on streamflow and sediment dynamics across the basin.

Table 2: Land-use change scenario for the Upper Cau River Basin by 2050, summarised from [34]

Land use type	Current 2020 (ha)	Planning by 2050 (ha)	Change (ha)	Change (%)
Rice	31,588.90	25,236.69	-6,352.21	-1.92
Forest	246,974.64	236,086.89	-10,887.75	-3.30
Other agricultural land	16,985.43	15,803.93	-1,181.50	-0.36
Residential	23,130.56	29,353.95	6,223.39	1.89
Non-agricultural land	8,760.28	21,657.05	12,896.78	3.91
Un-used lands	2,601.96	1,903.26	-698.70	-0.21
Total	**330,041.77**	**330,041.77**		

Table 3: Four simulation scenarios combining climate and land-use datasets for different time periods

Scenarios	Climate data	Land-use data
Baseline (S1)	1990 - 2020	2020
Land use change (S2)	1990 - 2020	2050
Climate change (S3)	2021 - 2050	2020
Combined (S4)	2021 - 2050	2050

3.3.3 Simulation scenarios

In this study, four scenarios were simulated using the SWAT model to assess the impacts of land-use and climate changes on streamflow and sediment yield (Table 3).

- *Baseline scenario (S1):* Using observed meteorological data (rainfall and temperature) for 1990-2020 and the current 2020 land-use data. This scenario served as the reference period and was used for model calibration and validation.
- *Land-use change scenario (S2):* Using land-use planning data by 2050 while maintaining historical climate conditions. This scenario evaluated the effects of agricultural and forest land conversion to urban and non-agricultural uses on streamflow and sediment yield.
- *Climate change scenario (S3):* Using projected climate data for 2021-2050 under the SSP2-4.5 scenario, combined with the current 2020 land-use data. This scenario isolates the influence of changes in rainfall and temperature on hydrological and sediment processes.
- *Combined scenario (S4):* Integrating both the land-use change and climate projections by 2050 to assess the combined impacts on future streamflow and sediment transport. Scenario S3 represents the isolated effects of future climate change with land use held constant at baseline conditions, whereas Scenario S4 captures the combined effects of future climate change and planned land-use change, allowing attribution of additional impacts to their interaction.

3.4 Soil Erosion Projection and Hotspot Identification

In SWAT, rainfall- and runoff-induced soil erosion is estimated using the MUSLE approach, which derives daily sediment yield based on runoff characteristics [35] and [43]. It should be noted that MUSLE estimates sediment yield associated with surface runoff and does not explicitly account for mass-movement processes such as landslides, which may be important in steep mountainous terrain. In this study, SWAT was applied to simulate sediment yield at the HRU scale under various land-use and climate scenarios to evaluate current and future erosion risk in the Upper Cau River Basin. The model outputs were imported into a GIS environment, where erosion intensity (t/ha/year) was classified into four levels: low (<5 t/ha), moderate (5–10 t/ha), high (10–30 t/ha), and very high (>30 t/ha) [21]. The erosion severity thresholds were adopted from commonly used classifications in soil erosion assessment studies and national erosion risk guidelines, which have been widely applied in SWAT-based analyses in mountainous and tropical regions [4][44] and [45]. Spatial analyses were then conducted to determine the extent and distribution of each erosion category across the basin.

By comparing the baseline (S1) and future combined (S4) scenarios, spatial patterns of erosion change were identified at both the HRU and sub-basin scales, allowing the delineation of areas with a high risk of soil loss. These areas were defined as erosion hotspots and represent spatially explicit priority zones for soil conservation and sustainable land management planning.

4. Results and Discussions

4.1 SWAT Model Performance

Detailed results on model performance for the Upper Cau River Basin have been previously reported in [20] and [21]. Here, a concise summary is provided to confirm model reliability for the present scenario-based analysis. As shown in Table 4, the SWAT model demonstrated strong predictive capability for streamflow, with high *NSE* and R^2 values during both calibration (0.95) and validation (0.90–0.91), and low bias indicators. Sediment simulations showed satisfactory performance, with calibration *NSE* of 0.76 and validation *NSE* of 0.62, remaining within commonly accepted thresholds for sediment modelling in steep tropical basins. These results are comparable to previous SWAT applications in similar hydro-climatic settings [4] and [8]. The model adequately reproduced seasonal patterns of streamflow and sediment yield, capturing wet-season peaks and dry-season low flows (Figure 4). Some underestimation occurred during major flood years (e.g., 2001, 2013, 2017), a known limitation in sediment modelling in steep tropical watersheds where episodic mass movements and channel-bank failures are not fully represented by HRU-scale MUSLE formulations [11] and [12].

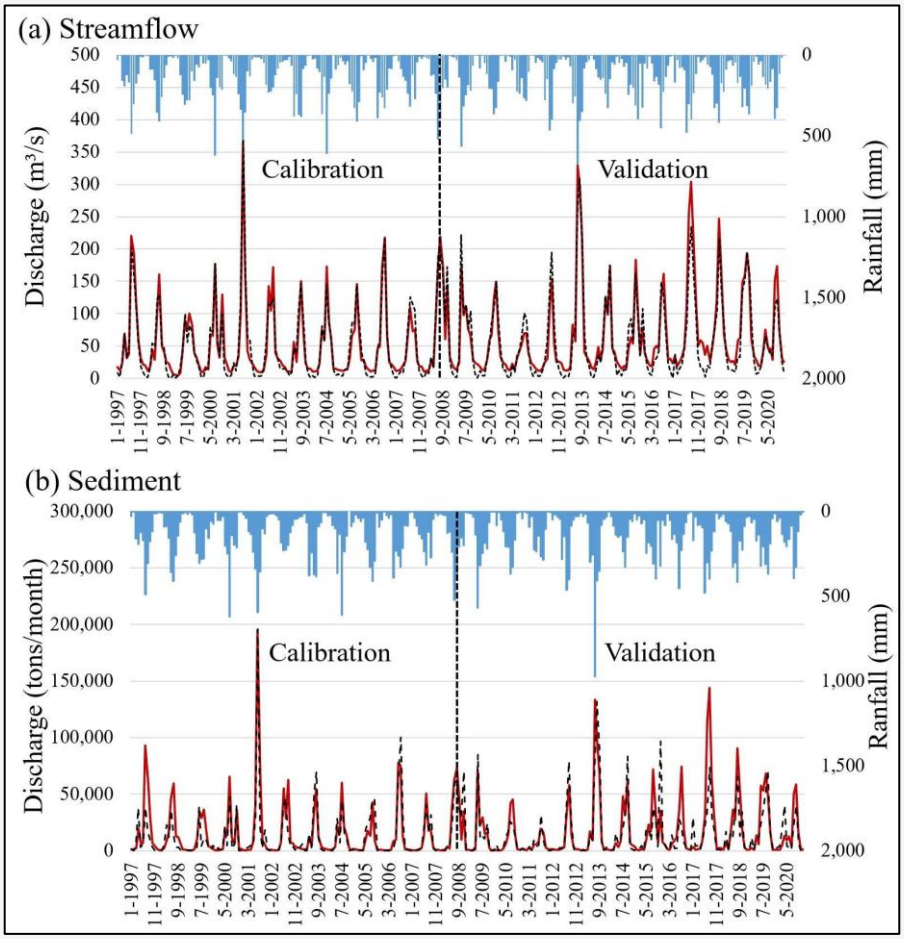

Figure 4: Comparison between observed and simulated monthly: (a) streamflow and (b) sediment yield during the calibration and validation periods at the Gia Bay station (adopted from [20] and [21])

Table 4: SWAT model performance during the calibration (1997-2008) and validation (2009-2020) periods

Variable	Period	R^2	*NSE*	*PBIAS* (%)	*RSR*
Streamflow	Calibration	0.95	0.95	2.60	0.23
	Validation	0.91	0.90	9.70	0.35
Sediment yield	Calibration	0.77	0.76	12.0	0.49
	Validation	0.63	0.62	-15.10	0.62

Nevertheless, the model reliably represents seasonal and interannual variability, providing a sound basis for evaluating future climate and land-use scenarios. A list of selected parameters and the results of the sensitivity analysis are presented in Table A2 and Figure A1.

4.2 Impacts of Climate and Land-Use Scenarios on Hydrology and Sediment Processes

4.2.1 Streamflow and surface runoff

Simulation results revealed substantial variations in streamflow and surface runoff across the four scenarios (Table 5 and Figure 5). Under the baseline scenario (S1), the mean streamflow discharge was 64.05 m³/s, with the wet season (111.4 m³/s) dominating over the dry season (16.7 m³/s). The highest flow (379.6 m³/s) occurred in July 2001, while the minimum (0.49 m³/s) was recorded in February 1996. Surface runoff was near-zero during the dry season but spiked for several years such as 1995, 2001 and 2013 (Figure 5(a)). When considering land-use change (S2), the mean streamflow discharge increased slightly by 0.82% (64.58 m³/s), primarily during the dry season (increased by 1.75%) and the seasonal transition months (February-April, increased by 4-6%), while

wet-season flow remained largely unchanged. Surface runoff rose by 10-20% in most months, though peak flood discharges slightly increased by 0.4%. This increase in surface runoff mainly reflects enhanced quick-flow generation, whereas baseflow contributions remained relatively stable, thereby offsetting the effect on total streamflow and resulting in only minor changes in monthly discharge.

Under the climate change scenario (S3), assuming land use remained at 2020 conditions, mean streamflow discharge increased markedly to 92.77 m³/s, representing a 44.83% increase relative to the baseline scenario (S1), with a maximum of 577.7 m³/s and a minimum of 0.70 m³/s. Mean surface runoff reached 34.39 mm/month (+6.14%), with peak monthly values up to 394.5 mm. When both climate change and land-use change were considered under the combined scenario (S4), mean streamflow increased slightly further to 92.84 m³/s, corresponding to a 44.95% increase compared to S1 and marginally exceeding S3. Peak discharge rose to 581.4 m³/s, exceeding both S3 and S1, while minimum discharge declined slightly to 0.68 m³/s, remaining 38.44% higher than S1. Mean surface runoff increased more substantially to 38.83 mm/month (+19.85% vs. S1; +6.5% vs. S2; +12.9% vs. S3), with a wet-season maximum of 419.24 mm, considerably higher than the corresponding value under S1 (282.15 mm). These results indicate that climate change is the dominant driver of changes in basin-scale streamflow, while the combined scenario (S4) leads to a nonlinear amplification of runoff and peak flow responses, particularly during wet-season conditions, reflecting enhanced quick-flow generation under concurrent climatic and land-surface changes.

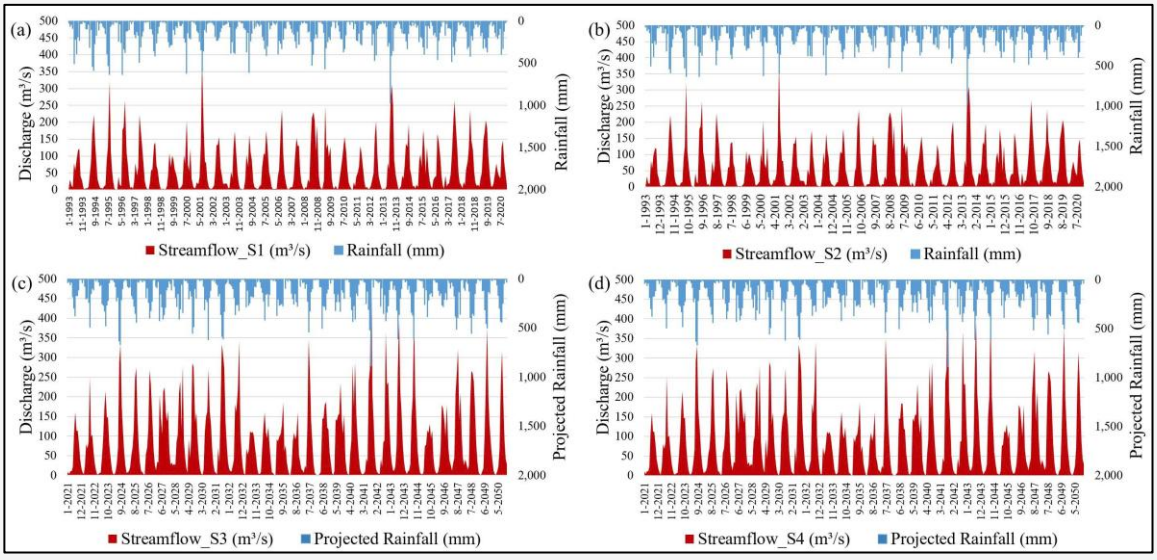

Figure 5: Monthly variations in streamflow under scenarios: (a) S1, (b) S2, (c) S3, and (d) S4

Table 5: Summary statistics of streamflow and surface runoff under different simulation scenarios. Δ% values indicate percentage changes relative to the baseline scenario (S1)

Variable	Metric	Scenario			
		Baseline (S1)	**Land-use change (S2)**	**Climate change (S3)**	**Combined (S4)**
Streamflow discharge (Q)	$\bar{Q}$ (m³/s)	64.05	64.58	92.77	92.84
	$\Delta\bar{Q}$ (%)	-	0.82	44.83	44.95
	Q_{max} (m³/s)	379.60	381.10	577.70	581.40
	Q_{min} (m³/s)	0.49	0.49	0.70	0.68
Surface runoff (Q_{surf})	$\bar{Q}_{surf}$ (mm)	32.40	36.47	34.39	38.83
	$\Delta\bar{Q}_{surf}$ (%)	-	12.56	6.14	19.85
	Q_{surf_max} (mm)	282.15	300.65	394.50	419.24
	Q_{surf_min} (mm)	0.00	0.00	0.00	0.00

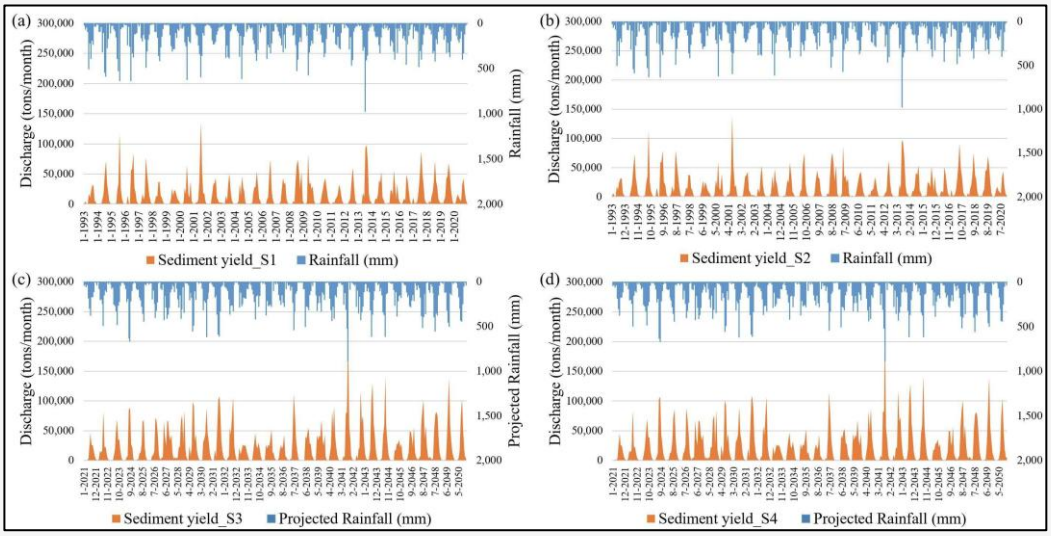

Figure 6: Monthly variations in sediment yield under scenarios (a) S1, (b) S2, (c) S3, and (d) S4

Table 6: Summary statistics of sediment discharge and yield under different simulation scenarios. Δ% values indicate percentage changes relative to the baseline scenario (S1)

Variable	Metric	Scenario			
		Baseline (S1)	**Land-use change (S2)**	**Climate change (S3)**	**Combined (S4)**
Sediment discharge (*Sed*)	$\overline{Sed}$ (t/month)	16,251.94	16,514.13	24,196.54	24,917.42
	$\Delta\overline{Sed}$(%)	-	1.61	48.88	53.32
	Sed_{max} (t/month)	135,000	137,400	209,100	211,600
	Sed_{min} (t/month)	30.57	9.11	6.86	14.32
Sediment yield (*SE*)	$\overline{SE}$ (t/ha/year)	2.62	9.56	4.55	12.57
	$\Delta\overline{SE}$ (%)	-	264.89	73.66	379.77
	SE_{max} (t/ha/year)	10.15	132.74	16.04	132.51
	SE_{min} (t/ha/year)	0.01	0.58	0.01	1.48

4.2.2 Sediment discharge and yield

The impacts of climate and land-use scenarios on sediment dynamics are presented in Table 6 and Figure 6. The baseline scenario (S1) showed a mean sediment discharge of 16.25×10³ t/month, with 91.7% transported during the wet season (29.8×10³ t/month) and only 2.7×10³ t/month in the dry season. The peak sediment discharge coincided with the July 2001 flood (135×10³ t/month). At the basin level, average sediment yield reached 2.62 t/ha/year, with several sub-basins (e.g., 50, 57, 59, 61, 66, 67) exceeding 5-10 t/ha/year. Under the land-use change scenario (S2), mean sediment discharge increased slightly to 16.5×10³ t/month (+1.61% compared to S1), while sediment yield rose sharply to 9.56 t/ha/year (+265% vs S1). About 78% of sub-basins showed increased sediment yield, notably sub-basins 38 (+126 t/ha/year), 30 (+77), 5 (+31), 46 (+26), and 47 (+17). In the climate scenario (S3), the mean sediment discharge reached 24.20×10³ t/month (+48.88% vs S1), with a maximum of 209.1×10³ t/month and a minimum of 6.86 t/month. Average sediment yield increased to 4.55 t/ha/year (+73.7% vs S1), particularly in sub-basins 50, 59, and 63.

The combined scenario (S4) produced the most pronounced effects. Mean sediment discharge reached 24.92×10³ t/month (+53.32% vs S1; +3% vs S3), with a peak of 211.6×10³ t/month. Average sediment yield surged to 12.57 t/ha/year (+380% vs S1; +31.5% vs S2; +176% vs S3). Several sub-basins experienced dramatic increases; for instance, sub-basin 30 (increased from 2.49 to 80.84 t/ha/year), 38 (increased from 6.45 to 132.51 t/ha/year), and 46 (increased from 1.43 to 31.75 t/ha/year). The land-use change scenario (S2) revealed a minimal impact on overall streamflow, reinforcing findings from previous studies that moderate forest reduction or urban expansion when climate inputs remain unchanged typically alters intra-annual flow distribution rather than annual water yield and [19]

and [46]. In contrast, sediment yield responded strongly, demonstrating the sensitivity of erosion processes to land-use transitions. This strong sediment response aligns with global tropical studies showing that even partial forest removal markedly increases soil detachment and sediment delivery on steep, weathered terrains [5] and [7]. Similar patterns have been reported in northern Vietnam, where soil structure is fragile and intensively weathered, causing rapid erosion following forest degradation [21] and [29]. Sub-basins with expanded bare, agricultural, or built-up areas experienced the highest increases some exceeding 130 t/ha/year comparable to erosion rates observed in degraded tropical highlands in Brazil, China, and the Himalayan foothills [6] and [13]. These results therefore highlight the disproportionate influence of land-use alteration on sediment responses relative to hydrological responses.

Climate change alone (S3) produced significant increases in streamflow and sediment yield, confirming that climate dynamics will be the primary driver of hydrological alteration in the Upper Cau River Basin. This finding reflects the projected intensification of rainfall under the SSP2-4.5 pathway, consistent with regional studies using CMIP6 datasets [17] and [22]. Similar hydrological amplification under climate change has been reported in major monsoon-dominated river systems such as the Jinsha, Mekong, and Upper Indus basins [9][11] and [13]. These studies likewise attribute increased flood peaks and sediment surges to more intense and frequent extreme rainfall events. The 73.7% increase in sediment yield under S3 aligns with the mechanistic understanding that rainfall erosivity rather than land cover is the primary driver of erosional processes during extreme events [12]. Thus, even in the absence of land-use change, future climate regimes alone will substantially intensify hydrological extremes and sediment transport.

The combined scenario (S4) exhibited the strongest and most nonlinear responses, demonstrating synergistic interactions between climate intensification and landscape modification. While streamflow changes in S4 remained similar to S3, indicating climate dominance, sediment yield increased nearly fourfold relative to S1, surpassing the increases observed in S2 (265%) and S3 (73.7%). This multiplicative response is consistent with studies from Kenya [8], the Brazilian Cerrado [6], and southwest China [47], all of which emphasized that simultaneous land-use degradation and rainfall intensification produce disproportionately high sediment outputs. The synergistic effect likely results from four reinforcing mechanisms: (i) higher rainfall intensity and runoff energy enhances detachment; (ii) reduced vegetation cover lowers soil resistance; (iii) expanded impervious or disturbed surfaces accelerate overland flow; and (iv) steep terrain increases sediment transport efficiency. These combined forces create feedback where climate-driven peaks mobilise larger volumes of sediment from increasingly exposed surfaces. Such dynamics have been documented in tropical montane basins under concurrent anthropogenic and climatic change [7] and [12].

4.3 Soil Erosion Projection and Hotspot Identification

As shown in Figure 7(a) and Table 7, under the baseline scenario (S1), areas with low erosion dominated the basin, covering 155,544 ha (47.13%), while moderate erosion accounted for 128,806 ha (39.03%). High erosion areas covered 31,505 ha (9.54%) and were mainly concentrated in sub-basins 61 and 63, whereas very high erosion occupied 14,187 ha (4.30%), notably in sub-basins 29 and 50, which were identified as current erosion hotspots. Under the combined scenario (S4), erosion intensity increased substantially across the basin (Figure 7(b) and Table 7). The extent of low-erosion areas declined sharply to 62,257 ha (18.86%), remaining primarily in sub-basins 40 and 41, where favourable topographic and vegetation conditions persist. In contrast, moderate erosion expanded considerably to 186,302 ha (56.45%), covering more than half of the basin and extending into several sub-basins previously classified as low risk, such as sub-basins 6 and 15. High-erosion areas also increased, reaching 54,877 ha (16.63%), with pronounced expansion observed in sub-basins 18, 20, and 24. Notably, very high erosion nearly doubled to 26,606 ha (8.06%) and became concentrated mainly in sub-basins 29, 38, 50, and 55.

Table 7: Summary of soil erosion levels under the baseline (S1) and combined (S4) scenarios

Erosion level	Scenario S1		Scenario S4	
	Area (ha)	Proportional area (%)	Area (ha)	Proportional area (%)
Low erosion	155,544	47.13	62,257	18.86
Moderate erosion	128,806	39.03	186,302	56.45
High erosion	31,505	9.54	54,877	16.63
Very high erosion	14,187	4.30	26,606	8.06

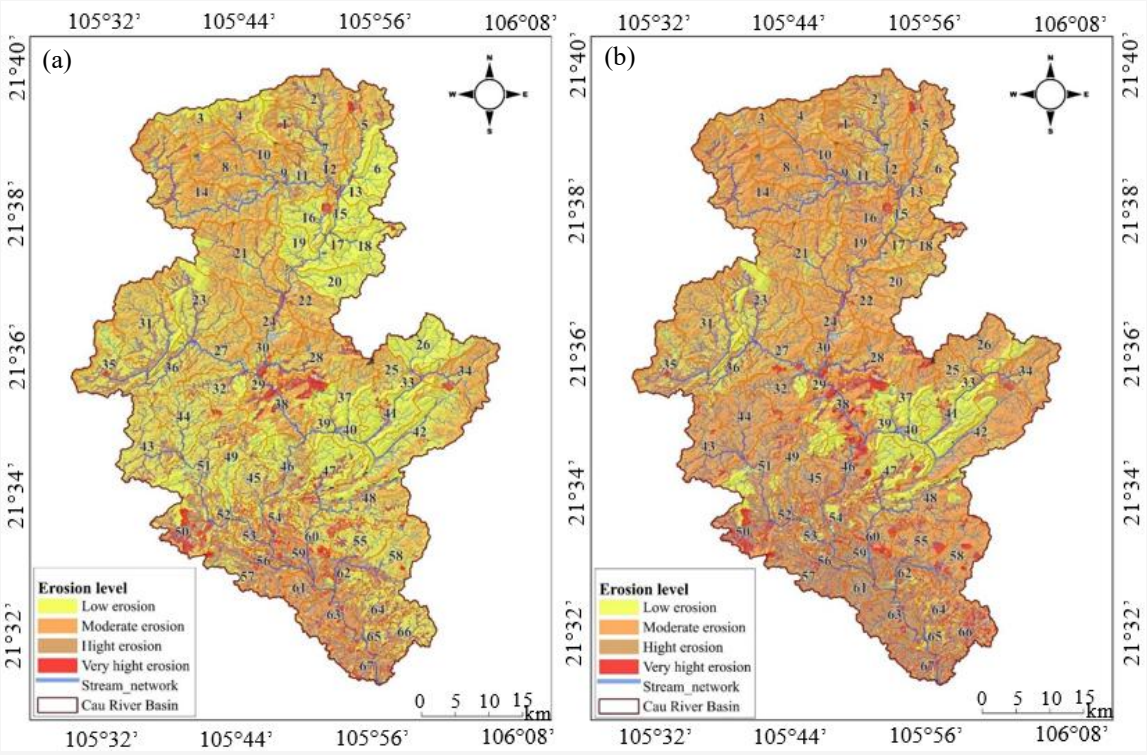

Figure 7: Spatial distribution of soil erosion under scenarios: (a) S1, and S4 (b) by HRU

Overall, both quantitative indicators and spatial patterns indicate a basin-wide transition from predominantly low-erosion conditions under S1 to moderate-to-high erosion dominance under S4. This pattern is consistent with empirical evidence showing that climate intensification disproportionately affects landscapes already weakened by land-use pressure [11] and [13]. The identified hotspot sub-basins share characteristics typical of high-risk tropical mountain systems: steep slopes, fragile soils, extensive forest loss, and expanding built-up areas. Similar spatial transitions have been reported in deforested regions of northern Laos, southwest China, and southern India, where erosion hotspots tend to migrate upslope or expand outward under combined climatic and anthropogenic influences. These findings highlight the importance of geographically targeted conservation measures rather than uniform basin-wide interventions.

The results provide robust evidence that combined climate and land-use pressures will substantially intensify soil erosion, sedimentation, and associated flood hazards. Effective mitigation therefore requires coordinated, forward-looking watershed governance. Key management implications include strengthening forest protection and restoration, particularly in steep upstream areas, to reduce runoff generation and stabilise soils. Conservation agriculture practices, such as contour farming and the use of cover crops, should be promoted to minimise erosion in areas undergoing agricultural expansion. Hotspot sub-basins identified in this study should be prioritised for targeted interventions within a sub-watershed planning framework. In addition, hydraulic infrastructure, including reservoirs and drainage systems, may need to be designed or upgraded to accommodate the higher sediment loads projected under the combined (S4) scenario. Finally, land-use management and climate adaptation policies should be integrated, recognising that future sediment risks arise from the combined influence of both drivers.

5. Conclusion

This study applied an integrated GIS–SWAT modelling framework to project and compare the individual and combined effects of climate change and land-use change on hydrological processes, sediment transport, and soil erosion in the upper area of the Upper Cau River Basin. The results demonstrate that while individual drivers alter basin dynamics, their combined effects produce substantially amplified hydrological and sediment responses. Under the combined scenario, mean streamflow increased by approximately 45%, sediment discharge at the basin outlet rose by over 53%, and basin-wide soil erosion exceeded baseline conditions by more than 379%, indicating a

substantial amplification of hydrological extremes when climate variability and land-use transitions occur simultaneously. Spatial analysis at both the HRU and sub-basin scales indicated a basin-wide shift from predominantly low erosion under S1 (47.13% of the basin area) to widespread moderate and high erosion under S4, with moderate erosion alone expanding to 56.45% of the basin area. These findings directly address the research gap regarding the compound influence of climate and land-use change in mountainous tropical watersheds.

From a watershed management perspective, the projected intensification of runoff and sediment mobilisation suggests growing risks of flash flooding, channel instability, and reservoir sedimentation in the Cau River system. Spatial hotspot analysis further reveals that erosion risks are concentrated in specific steep sub-basins where forest loss and hydrological connectivity interact. These areas should be prioritised for targeted management interventions, including slope stabilisation, reforestation corridors, and soil conservation practices linked to local land-use zoning and watershed planning. Overall, this study highlights the importance of integrating climate and land-use scenarios when evaluating future hydrological risks. The combined modelling and spatial hotspot identification framework can provide a transferable approach for identifying priority intervention zones in mountainous watersheds of northern Vietnam and similar environments. Future research should incorporate multi-model climate ensembles and improved sediment process representation to better characterise uncertainty and support climate-resilient watershed management strategies.

6. Limitations

Despite the robust performance of the SWAT model in simulating streamflow and sediment dynamics in the Upper Cau River Basin, several limitations and sources of uncertainty should be acknowledged. First, model calibration and validation relied on a single long-term hydrological station (Gia Bay), which constrained internal sub-basin validation and may limit representation of spatial variability in hydrological and sediment responses across the basin. Similarly, the density of meteorological stations, although representative of major elevation and climatic gradients, remains limited for a complex mountainous watershed.

Second, future climate projections were derived from a single global climate model (UKESM1-0-LL) under the SSP2-4.5 scenario. While this model has demonstrated favourable performance over Southeast Asia, the use of a single GCM does not fully capture the range of uncertainty associated with multi-model climate ensembles. Consequently, the magnitude of projected hydrological and erosion responses should be interpreted as scenario-specific rather than probabilistic estimates.

Third, sediment yield was simulated using the MUSLE method, which estimates erosion driven by surface runoff but does not explicitly represent mass-movement processes such as landslides and debris flows. In steep mountainous sub-basins, particularly under extreme rainfall events, these processes may contribute additional sediment loads beyond those simulated by MUSLE, potentially leading to underestimation of extreme erosion values.

Finally, land-use change scenarios were based on officially adopted planning maps, which provide policy-relevant and spatially explicit projections but inherently assume successful implementation of planned land-use transitions. Deviations from planned development pathways or unregulated land-use changes could result in different hydrological and erosion outcomes. Despite these limitations, the integrated GIS–SWAT framework applied in this study provides valuable insights into the relative and combined impacts of climate change and land-use change, and offers a scientifically grounded basis for spatial prioritization and adaptive watershed management.

Funding

This work was financially supported by Vietnam Ministry of Education and Training under project number: B2024-TNA-15.

Acknowledgments

We would like to express our deepest gratitude and remembrance for Associate Professor Phan Dinh Binh (Faculty of Resource Management, University of Agriculture and Forestry - Thai Nguyen University), who initiated the research idea and was the original principal investigator of this project. Although he sadly passed away, his invaluable contributions and unwavering dedication remain a foundational part of this study and continue to inspire its completion.

References

[1] Wang, W., Shao, Q., Yang, T., Peng, S., Xing, W., Sun, F. and Luo, Y., (2013). Quantitative Assessment of the Impact of Climate Variability and Human Activities on Runoff Changes: A Case Study in Four Catchments of the Haihe River Basin, China. *Hydrological Processes*, Vol. 27(8), 1158-1174. https://doi.org/https://doi.org/10.1002/hyp.9299.

[2] Ngo, A., Grivel, S., Nguyen, T. and Nguyen, T., (2023). Impact Assessment of Land Use and Land Cover Change on the Runoff Changes on the Historical Flood Events in the Laigiang River Basin of the South Central Coast Vietnam. *International Journal of Geoinformatics*, Vol. 19(10), 51-63. https://doi.org/10.52939/ijg.v19i9.2881.

[3] Alshammari, E., Rahman, A. A., Ranis, R., Seri, N. A. and Ahmad, F., (2024). Investigation of Runoff and Flooding in Urban Areas Based on Hydrology Models: A Literature Review. *International Journal of Geoinformatics*, Vol. 20(1), 99-119. https://doi.org/10.52939/ijg.v20i1.3033.

[4] Thai, T. H., Thao, N. T. P. and Dieu, B. T., (2017). Assessment and Simulation of Impacts of Climate Change on Erosion and Water Flow by Using the Soil and Water Assessment Tool and Gis: Case Study in Upper Cau River Basin in Vietnam. *Vietnam Journal of Earth Sciences*, Vol. 39, 376-392.

[5] Neill, C., Deegan, L. A., Thomas, S. M. and Cerri, C. C., (2001). Deforestation for Pasture Alters Nitrogen and Phosphorus in Small Amazonian Streams. *Ecological Applications*, Vol. 11(6), 1817-1828. https://doi.org/10.2307/3061098.

[6] de Paulo Rodrigues da Silva, V., Silva, M. T., Singh, V. P., de Souza, E. P., Braga, C. C., de Holanda, R. M., Almeida, R. S. R., de Assis Salviano de Sousa, F. and Braga, A. C. R., (2018). Simulation of Stream Flow and Hydrological Response to Land-Cover Changes in a Tropical River Basin. *Catena*, Vol. 162, 166-176. https://doi.org/https://doi.org/10.1016/j.catena.2017.11.024.

[7] Lucas-Borja, M. E., Carrà, B. G., Nunes, J. P., Bernard-Jannin, L., Zema, D. A. and Zimbone, S. M., (2020). Impacts of Land-Use and Climate Changes on Surface Runoff in a Tropical Forest Watershed (Brazil). *Hydrological Sciences Journal*, Vol. 65(11), 1956-1973. https://doi.org/10.1080/02626667.2020.1787417.

[8] Mango, L. M., Melesse, A. M., McClain, M. E., Gann, D. and Setegn, S. G., (2011). Land Use and Climate Change Impacts on the Hydrology of the Upper Mara River Basin, Kenya: Results of a Modeling Study to Support Better Resource Management. *Hydrology and Earth System Sciences*, Vol. 15(7), 2245-2258. https://doi.org/10.5194/hess-15-2245-2011.

[9] Seeboonruang, U., Mandadi, R., Thammaboribal, P., Gonzales, A. L., and Bharadwaz, G. S. V. S. A. (2025). Estimation of Soil Erosion and Enhancing Sediment Retention in the Lam Phra Phloeng Watershed: Insights from RUSLE and InVEST Modelling. *Water*. Vol. 17(23);3339. https://doi.org/10.3390/w17233339.

[10] Kulsoontornrat, J. and Puangkaew, N., (2025). Assessing the Impacts of Land Use and Land Cover Changes on Sediment Yield Using the Swat Model: A Case Study in the Khlong Bang Yai Watershed, Phuket Island, Thailand. *International Journal of Geoinformatics*, Vol. 21(5), 62-79. https://doi.org/10.52939/ijg.v21i5.4161.

[11] Penny, J., Khadka, D., Babel, M., Alves, P., Djordjević, S., Chen, A. S. and Loc, H. H., (2023). Integrated Assessment of Flood and Drought Hazards for Current and Future Climate in a Tributary of the Mekong River Basin. *Journal of Water and Climate Change*, Vol. 14(12), 4424-4443. https://doi.org/10.2166/wcc.2023.252.

[12] Owens, P. N., (2020). Soil Erosion and Sediment Dynamics in the Anthropocene: A Review of Human Impacts During a Period of Rapid Global Environmental Change. *Journal of Soils Sediments*, Vol. 20(12), 4115-4143. https://doi.org/10.1007/s11368-020-02815-9.

[13] Seeboonruang, U., Mandadi, R., Thammaboribal, P., Gonzales, A. L., Kanchan, A., and Ganni, S. V. S. A. B., (2025). Assessing the Combined Impacts of Future Climate and Land Use Changes on Soil Loss and Sediment Retention in the Lam Phra Phloeng Watershed, Thailand. *Agriculture*. Vol. 15(23). https://doi.org/10.3390/agriculture15232511.

[14] Taran, A., Al-Ghumaid, A. and Al-Mayouf, F., (2021). Assessing the Hydrological and Sedimentary Reality of Amman/Zarqa Basin Using the Soil and Water Assessment Tool. *International Journal of Geoinformatics*, Vol. 17(6), 71-84. https://ijg.e-geoinfo.com/index.php/journal/article/view/2069.

[15] Arnold, J. G., Srinivasan, R., Muttiah, R. S. and Williams, J. R., (1998). Large Area Hydrologic Modeling and Assessment Part I: Model Development 1. *JAWRA Journal of the American Water Resources Association*, Vol. 34(1), 73-89. https://doi.org/10.1111/j.1752-1688.1998.tb05961.x.

[16] Tong, S. T. Y., Sun, Y., Ranatunga, T., He, J. and Yang, Y. J., (2012). Predicting Plausible Impacts of Sets of Climate and Land Use Change Scenarios on Water Resources. *Applied Geography*, Vol. 32(2), 477-489. https://doi.org/10.1016/j.apgeog.2011.06.014.

[17] Ministry of Natural Resources and Environment, (2009). *Climate Change, Sea Level Rise Scenarios for Vietnam* ". Ministry of Natural Resources and Environment, Hanoi, Vietnam.

[18] Van Trinh, M., (2007). *Soil Erosion and Nitrogen Leaching in Northern Vietnam: Expression and Modelling* Wageningen University]. Wageningen, The Netherlands.

[19] Khoi, D. N. and Suetsugi, T., (2014). Impact of Climate and Land-Use Changes on Hydrological Processes and Sediment Yield-a Case Study of the Be River Catchment, Vietnam. *Hydrological Sciences Journal*, Vol. 59(5), 1095-1108. https://doi.org/10.1080/02626667.2013.819433.

[20] Nguyen, N. A., Chu, V. T., Nguyen, L. H., Ha, A. T. and Nguyen, T. H., (2025). Streamflow Simulation in the Cau River Basin, Northeast Vietnam, Using Swat-Based Hydrological Modelling. *Geographies*, Vol. 5(3). https://doi.org/10.3390/geographies5030041.

[21] Nguyen, N. A., Chu, V. T., Nguyen, T. H. and Nguyen, H. T., (2026). Spatio-Temporal Dynamics of Soil Erosion and Its Relationship with Forest Loss in the Upper Cau River Basin, Northern Vietnam. *Hydrological Sciences Journal*, Vol. 1, 20-30. https://doi.org/10.1080/02626667.2026.2641056.

[22] Tran-Anh, Q., Ngo-Duc, T., Espagne, E. and Trinh-Tuan, L., (2023). A 10-Km Cmip6 Downscaled Dataset of Temperature and Precipitation for Historical and Future Vietnam Climate. *Scientific Data*, Vol. 10(1), 257. https://doi.org/10.1038/s41597-023-02159-2.

[23] Bach, T. V., (2017). Application of the Swat Model for Simulating Streamflow and Sediment Yield. *Journal of Water Resources and Environmental Engineering*, Vol. 57, 136-142.

[24] Ministry of Natural Resources and Environment, (2006). *Vietnam National Environmental Report 2006: Status of Three Water Basin: Cau River, Nhue – Day River and Dong Nai River* ". Ministry of Natural Resources and Environment, Hanoi, Vietnam.

[25] Quy, L. D., (1990). Developing Flood Inundation Maps of Bac Thai Caused by Flooding from the Cau River and Cong River. *Journal of Meteorology and Hydrology*, Vol. 2(353), 15-23.

[26] National Centers for Environmental Information (NCEI), (2025). *Monthly Climate Reports: Tropical Cyclones – October 2025* [Monthly climate report]". National Oceanic and Atmospheric Administration, National Oceanic and Atmospheric Administration. Accessed: 31 January 2026. [Online]. Available: https://www.ncei.noaa.gov/access/monitoring/monthly-report/tropical-cyclones/202510.

[27] Duong Thi, L., Do Van, T. and Le Van, H., (2020). Detection of Flash-Flood Potential Areas Using Watershed Characteristics: Application to Cau River Watershed in Vietnam. *Journal of Earth System Science*, Vol. 129(1). https://doi.org/10.1007/s12040-020-01386-0.

[28] Jimenez, J., Tripathi, N., Pandey, A., Shrestha, S., Chao, K., Gatela Jr, E., Jimenez Jr, J. and Aspiras, J., (2025). Geospatial Governance for Sustainable Water Resources Management: Integrating Swat Modeling, Satellite Data, and Hydrogeological Units in Padsan River Watershed. *International Journal of Geoinformatics*, Vol. 21(10). https://doi.org/10.52939/ijg.v21i10.4525.

[29] Thien, B. B., Phuong, V. T. and Huong, D. T., (2024). Forest Cover Depletion and Land Use/Land Cover Change in Bac Kan Province, Vietnam. *Geofocus: Revista Internacional de Ciencia y Tecnología de la Información Geográfica*, Vol. 34, 29-44. https://doi.org/10.21138/GF.820.

[30] Departments of Natural Resources and Environment of Thai Nguyen, (2021). *Assessment of Land Use Change in Thai Nguyen During 2011-2020* ". Thai Nguyen Province Government, Thai Nguyen, Vietnam.

[31] Sellar, A. A., Jones, C. G., Mulcahy, J. P., Tang, Y., Yool, A., Wiltshire, A., O'connor, F. M., Stringer, M., Hill, R. and Palmieri, J., (2019). Ukesm1: Description and Evaluation of the Uk Earth System Model. *Journal of Advances in Modeling Earth Systems*, Vol. 11(12), 4513-4558. https://doi.org/10.1029/2019MS001739.

32] Rabus, B., Eineder, M., Roth, A. and Bamler, R., (2003). The Shuttle Radar Topography Mission-a New Class of Digital Elevation Models Acquired by Spaceborne Radar. *ISPRS Journal of Photogrammetry and Remote Sensing*, Vol. 57(4), 241-262. https://doi.org/10.1016/S0924-2716(02)00124-7.

[33] Zandbergen, P., (2008). Applications of Shuttle Radar Topography Mission Elevation Data. *Geography Compass*, Vol. 2(5), 1404-1431. https://doi.org/10.1111/j.1749-8198.2008.00154.x.

[34] Thai Nguyen Province Government and Bac Kan Province Government, (2023). *Provincial Land-Use Planning Documents for Thai Nguyen and Bac Kan (2021–2030, Vision to 2050)* in "Official Provincial Planning Reports. [Online]. Available: https://ioc.thainguyen.gov.vn, https://www.mpi.gov.vn.

[35] Arnold, J., Moriasi, D., Gassman, P., Abbaspour, K., White, M., Srinivasan, R., Santhi, C., Harmel, R., van Griensven, A., Van Liew, M., Kannan, N. and Jha, M., (2012). Swat: Model Use, Calibration, and Validation. *Transactions of the ASABE (American Society of Agricultural and Biological Engineers)*, Vol. 55(4), 1491–1508. https://doi.org/10.13031/2013.42256.

[36] Wang, Y., Ziv, G., Adami, M., Mitchard, E., Batterman, S. A., Buermann, W., Schwantes Marimon, B., Marimon Junior, B. H., Matias Reis, S., Rodrigues, D. and Galbraith, D., (2019). Mapping Tropical Disturbed Forests Using Multi-Decadal 30 M Optical Satellite Imagery. *Remote Sensing of Environment*, Vol. 221, 474-488. https://doi.org/10.1016/j.rse.2018.11.028.

[37] Moradkhani, H. and Sorooshian, S., (2008). General Review of Rainfall-Runoff Modeling: Model Calibration, Data Assimilation, and Uncertainty Analysis. In: Hydrological Modelling and the Water Cycle: Coupling the Atmospheric and Hydrological Models, (S. Sorooshian, K.-L. Hsu, E. Coppola, B. Tomassetti, M. Verdecchia, and G. Visconti, Eds.). Springer Berlin Heidelberg. https://doi.org/10.1007/978-3-540-77843-1_1.

[38] Neitsch, S. L., Arnold, J. G., Kiniry, J. R. and Williams, J. R., (2005). Soil and Water Assessment Tool Theoretical Documentation Version 2005., ed, 2005. 1-494. https://swat.tamu.edu/media/1292/swat2005theory.pdf.

[39] Seeboonruang, U., Mandadi, R., Thammaboribal, P., Gonzales, A. L., Kanchan, A., Ganni, S. V. S. A. B., (2026). Land Use Classification, Prediction, and the Relationship Between Land Use and Sediment Loss in the Lam Phra Phlong Watershed, Thailand. *Agriculture*. Vol. 16, 448. https://doi.org/10.3390/agriculture16040448.

[40] Chakraborty, K., Saha, S. and Mandal, D., (2024). Hydrological Modelling Using Swat for the Assessment of Streamflow Dynamics in the Ganga River Basin. *Environmental SciencePollution Research*, 1-21. https://doi.org /10.1007/s11356-024-34385-5.

[41] Abbaspour, K. C., Rouholahnejad, E., Vaghefi, S., Srinivasan, R., Yang, H. and Kløve, B., (2015). A Continental-Scale Hydrology and Water Quality Model for Europe: Calibration and Uncertainty of a High-Resolution Large-Scale Swat Model. *Journal of Hydrology*, Vol. 524, 733-752. https://doi.org/10.1016/j.jhydrol.2015.03.027.

[42] Moriasi, D. N., Arnold, J. G., Van Liew, M. W., Bingner, R. L., Harmel, R. D. and Veith, T. L., (2007). Model Evaluation Guidelines for Systematic Quantification of Accuracy in Watershed Simulations. *Transactions of the ASABE*, Vol. 50(3), 885-900. https://swat.tamu.edu/media/1312/moriasimodeleval.pdf.

[43] Willams, J., (1975). *Sediment-Yield Prediction with Universal Equation Using Runoff Energy Factor*. In: Present Prospective Technology for Predicting Sediment Yields Sources, (Agriculture Research Service, Ed.). US Department of Agriculture.

[44] Dechasa, A., Aga, A. O. and Dufera, T., (2022). Erosion Risk Assessment for Prioritization of Conservation Measures in the Watershed of Genale Dawa-3 Hydropower Dam, Ethiopia. *Quaternary*, Vol. 5(4). https://doi.org/10.3390/quat5040039.

[45] National Technical Standards Committee, (2009). *Soil Quality – Method for Determination of Soil Erosion by Rain (Tcvn 5299: 2009)*. Ministry of Science and Technology, Hanoi, Vietnam.

[46] Ward, P. J., van Balen, R. T., Verstraeten, G., Renssen, H. and Vandenberghe, J., (2009). The Impact of Land Use and Climate Change on Late Holocene and Future Suspended Sediment Yield of the Meuse Catchment. *Geomorphology*, Vol. 103(3), 389-400. https://doi.org/10.1016/j.geomorph.2008.07.006.

[47] Xing, M., Xu, J., Luo, Y., Aggarwal, S. and Jiatong, L., (2009). Response of Hydrological Processes to Land-Cover and Climate Changes in Kejie Watershed, South-West China. *Hydrological Processes*, Vol. 23, 1179-1191. https://doi.org/10.1002/hyp.7233.

Appendix

Table A1: Summary of the key parameters included in the sensitivity analysis in SWAT-CUP

No.	Parameter	Description	Unit
Parameters for streamflow			
1	CN2.mgt	Curve number	-
2	ALPHA_BF.gw	Baseflow alpha factor	l/days
3	GW_DELAY.gw	Groundwater delay time	days
4	GWQMN.gw	Threshold depth of water in the shallow aquifer for return flow to occur	mm
5	SURLAG.bsn	Surface runoff delay time	days
6	ESCO.hru	Soil evaporation compensation factor	-
7	SOL_K(1).sol	Saturated hydraulic conductivity (topsoil layer)	mm/hr
8	SOL_AWC(1).sol	Available water capacity (topsoil layer)	mm/mm
9	REVAPMN.gw	Threshold depth of water in the shallow aquifer for “revap” to occur	mm
10	RCHRG_DP.gw	Deep aquifer percolation fraction	-
Parameters for sediment yield			
1	USLE_K(1).sol	USLE Soil erodibility (K) factor	t·ha·h/(MJ·mm)
2	USLE_P.mgt	USLE Support practice (P) factor	-
3	SLSUBBSN.hru	Slope length (m)	m
4	LAT_SED.hru	Concentration of sediment in lateral subsurface flow (mg/L)	-
5	CH_N2.rte	Manning’s roughness coefficient for the main channel	-
6	CH_K2.rte	Effective hydraulic conductivity of channel (mm/hr)	mm/hr
7	CH_COV1.rte	Channel erodibility factor	-

Table A2: Selected parameters along with their optimal calibrated values and the ranges obtained through calibration using SUFI-2.

Parameter	Fitted Value	Minimum	Maximum
r_CN2.mgt	-0.0628	-0.2	0.2
r_SOL_K(1).sol	-0.1010	-0.2	2.0
V_ESCO.hru	0.9042	0.8	1.0
r_SOL_AWC(1).sol	1.2058	-0.2	2.0
r_USLE_K(1).sol	-0.0870	-0.3	0.3
v_USLE_P.mgt	0.6607	0.1	1.0
r_SLSUBBSN.hru	0.4928	-0.3	0.5

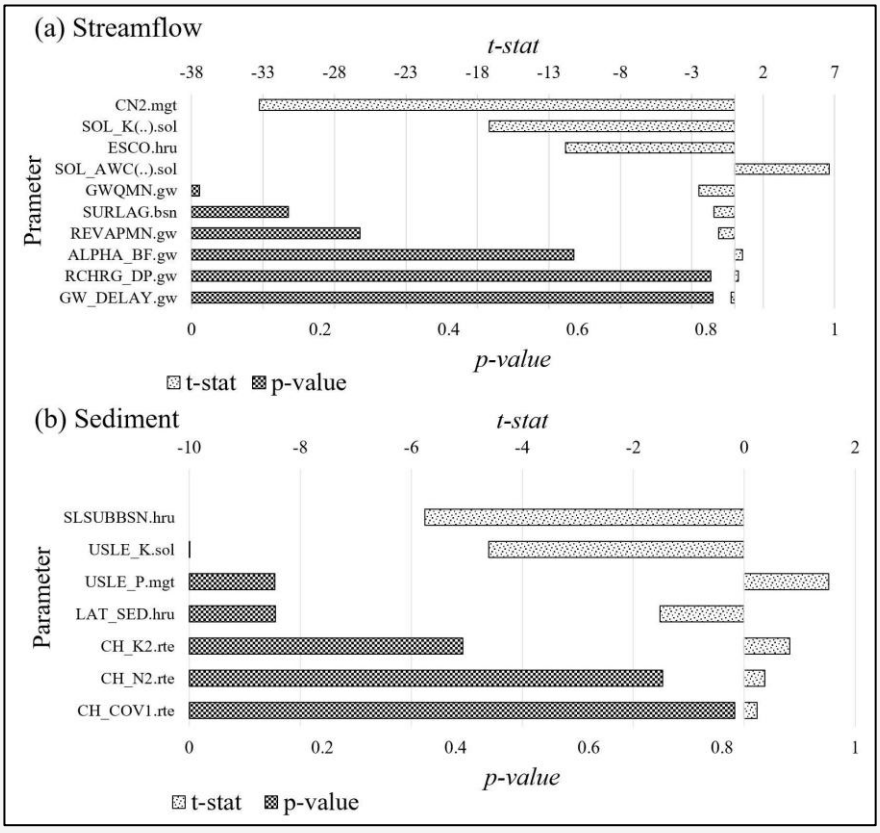

Figure A1: Sensitivity chart showing the t-stat and p-value for each parameter considered during the SWAT model calibration for (a) streamflow and (b) sediment